Highly Sensitive Waveguide Bragg Grating Temperature Sensor Using Hybrid Polymers

Nuria Teigell Benéitez, Jeroen Missinne, Yuting Shi, Gabriele Chiesura, Geert Luyckx, Joris Degrieck, and Geert Van Steenberge

***Abstract*— A waveguide Bragg grating temperature sensor implemented using a hybrid inorganic-organic material (Ormocer) with a 25-times higher temperature sensitivity than a typical silica fiber is presented. The sensor consists of second order gratings (1010-nm pitch) in 5 μm × 5 μm waveguides fabricated on a planar substrate using the replication-based methods. The gratings were imprinted in the under-cladding layer, and the waveguide cores were patterned on top by capillary filling of microchannels, which were defined in a transparent and flexible mold. The somewhat larger, slightly multimode waveguides facilitate pigtailing with an optical fiber but lead to three reflection peaks corresponding to the different excited waveguide modes. The peak at the longest wavelength (Bragg wavelength at 1539 nm, corresponding to the fundamental mode) was tracked during temperature testing, and a sensitivity of -249 pm $^{\circ}C^{-1}$ was found.**

***Index Terms*— Bragg grating, capillary filling, high sensitivity, imprinting, Ormocer, polymer waveguide, replication, temperature sensor.**

I. Introduction

TEMPERATURE sensors play an important role in different sectors and applications such as healthcare, consumer electronics, automotive, aerospace etc. The demand for high performance, reliable and low-cost temperature sensors is growing to satisfy the increasing automation needs in manufacturing and monitoring. There is a trend to integrate such sensors in materials (e.g. composites) during the fabrication process. In certain applications, traditional electronic-based temperature sensors are not suitable due to their susceptibility to electro-magnetic interference [1]. A particular type of optical sensors, based on Bragg gratings, represents a growing market segment owing to their simplicity, low cost and multiplexing capability. These Bragg gratings are mainly implemented in fibers, however, the silica thermo-optic coefficient is very low compared to other materials such as polymers [2], [3] which leads to a lower temperature sensitivity. Several efforts have been made to enhance the sensitivity of silica fiber sensors using additional transducer mechanisms [1], [4], [5]. For example, the results obtained in [4], reporting a sensitivity of 150 pm $^{\circ}C^{-1}$, were found to be comparable with the performance of polymers but several steps were required to deal with the inherent bad adhesion of Teflon. During the last years, work on polymer optical fibers (POFs) has significantly progressed and Bragg gratings have successfully been inscribed [6]–[12] leading to a typical temperature sensitivities ranging from -50 pm $^{\circ}C^{-1}$ to -100 pm $^{\circ}C^{-1}$.

As an alternative to fibers for sensing, optical waveguides on a planar substrate are interesting because additional functionality, such as splitters, optoelectronic components [13], or even complete Bragg grating interrogation systems [14] can be integrated. Furthermore, the use of planar foils facilitates orientation and positioning of the sensors during integration compared to discrete fiber sensors. Bragg grating-based sensors in polymer waveguides are gaining more and more interest in numerous applications [15]–[18] owing to the variety of available materials, each having specific properties and being optimized for certain fabrication methods. Ormocer, an inorganic-organic hybrid polymer, is a good candidate for implementing a Bragg grating-based temperature sensor because of its good thermal stability, relatively low absorption loss from visible to telecom wavelengths and high thermo-optic coefficient. Furthermore, the material is cost-effective, is easy to use and safe to handle without special protection. However, it is difficult to define micrometer size waveguide features using standard contact mask lithography due to its oxygen inhibition and liquid state during UV-exposure. As an alternative, an imprinting-based technology has been proposed [19], but the reported structures achieved with this technique are inverted-rib waveguides due to the rather thick residual layer.

Therefore, we report a new capillary filling-based replication method for fabricating a highly sensitive Ormocer-based waveguide Bragg grating temperature sensor. The sensor consists of a (set of) polymer waveguide(s) patterned on top of an under-cladding layer with a large area grating imprinted, which results in a sensitivity of -249 pm $^{\circ}C^{-1}$ around room temperature at an interrogation wavelength around 1530 nm.

II. Fabrication Methods

The fabrication of the sensor comprises two main steps i.e. (1) patterning of the grating on the Ormoclad cladding

Manuscript received November 3, 2015; revised February 10, 2016; accepted February 17, 2016. Date of publication February 23, 2016; date of current version March 29, 2016. This work was supported by the Flemish Government within the framework of the Project Self-Sensing Composites under Grant IWT SBO 120024.

N. Teigell Benéitez, J. Missinne, Y. Shi, and G. Van Steenberge are with the Centre for Microsystems Technology, imec, Ghent University, Ghent 9052, Belgium (e-mail: nuria.teigellbeneitez@elis.ugent.be; jeroen.missinne@elis.ugent.be; yuting.shi@ugent.be; geert.vansteenberge@elis.ugent.be).

G. Chiesura, G. Luyckx, and J. Degrieck are with the Department of Materials Science and Engineering, Ghent University, Ghent 9052, Belgium (e-mail: gachiesu.chiesura@ugent.be; geert.luyckx@ugent.be; joris.degrieck@ugent.be).

Color versions of one or more of the figures in this letter are available online at http://ieeexplore.ieee.org.

Digital Object Identifier 10.1109/LPT.2016.2533020

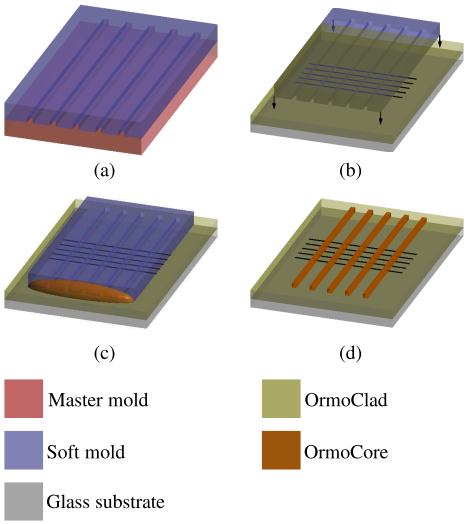

Fig. 1. Process flow showing the most important steps to define the waveguide cores on top of the grating-patterned under-cladding. (a) Fabrication of the soft mold. (b) Soft mold placed in contact with the cladding. (c) Capillary filling of the mold channels. (d) Mold releasing revealing the core structures.

layer and (2) the definition of the Ormocore waveguide core on top. Both materials are commercially available Ormocer formulations (Micro Resist Technology) with a refractive index difference of 0.02 at 1550 nm.

Gratings with a pitch of 1010 nm (second order reflections around telecom wavelengths) were first fabricated in a layer of AZ Mir 701 positive photoresist by phase mask lithography, serving as a master mold. A replicated soft mold was fabricated by casting a UV-curable transparent polymer (OF-134, MyPolymers) on top of the master mold and curing it with a UV lamp. The grating structure in the soft mold was then transferred to an Ormoclad layer spin-coated (30 s at 3000rpm) on a Borofloat glass substrate by placing the mold in contact with this layer taking care to avoid trapped air bubbles. The Ormoclad layer is then UV-cured under N_2 for 30 s at 30 mW cm^{-2} and then the soft mold is peeled off. The cladding with the transferred gratings was post baked (hot plate, 85 °C) and hard baked (convection oven, 150 °C) prior to processing the waveguide cores.

The waveguide cores were defined by capillary filling another soft mold with a mix of Ormocore and ma-T 1050 solvent (Micro Resist Technology) prepared in a 1:1 ratio by weight (selected as a trade-off between viscosity and limiting the amount of solvent). This soft mold for defining the waveguide cores was prepared analogously to the grating mold (Fig. 1 (a)) but using a master mold having 5 µm × 5 µm waveguides which were fabricated using laser direct-write lithography in an Epocore layer spin-coated on a silicon substrate. After peeling off the soft mold from the master mold, a razor blade was used to open the waveguide channels. The soft mold was then placed on top of the under-cladding with the gratings (Fig. 1 (b)), a drop of the Ormocore-solvent mixture was placed in contact with one side of the open channels (Fig. 1 (c)) and the sample was allowed to rest (about 1 hour) until the required length was filled. A UV-curing step for 2 minutes at 30 mW cm^{-2} was then performed in a N_2 chamber and afterwards the mold was released (Fig. 1 (d)).

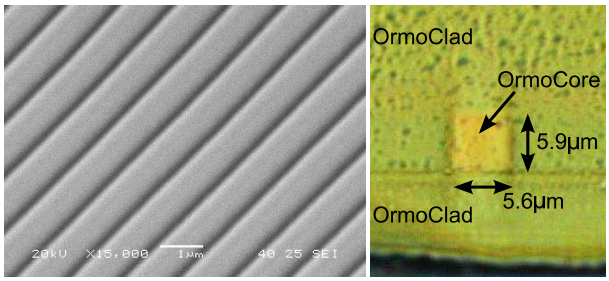

Fig. 2. SEM micrograph of the grating transferred to the Ormoclad under-cladding (left). Cross-sectional view of an Ormocore waveguide fabricated by capillary filling (right).

Finally, the Ormocore waveguides were hard-baked and covered with an Ormoclad cladding layer using spin-coating.

After processing, the sample was diced with a DAD 322 Disco Automatic wafer dicer at 10 000rpm and 1 mm s^{-1} to obtain optically-clear end-faces. To test the sensor in a relevant environment, an SMF-28 single mode optical fiber was pigtailed to one of the waveguides using a UV-curable epoxy. On the other end-face of the waveguide, a drop of this glue was used to reduce parasitic reflections.

III. Results and Discussion

A. Fabrication Results

The gratings imprinted in Ormoclad were visually inspected using a microscope and SEM, showing a good replication quality and grating uniformity over a large area, see Fig. 2. After the waveguide cores were defined, the sample was visualized under the microscope showing defect-free waveguides and the proper filling of the channels both in the regions with and without gratings. Manual positioning the soft mold only leads to a angular misalignment of about 1° between grating and waveguide. As can be seen from the cross-section of an Ormocore waveguide (covered with cladding) shown in Fig 2, the capillary filled cores presented the same rectangular shape as the soft mold, meaning that the channels were filled over their complete cross-section and that no significant shrinkage was observed during the UV-curing process. Using this capillary filling technique, waveguides with a total length of 1 cm to 2 cm can be obtained, which is sufficient for implementing temperature sensors. For other applications that require longer waveguides, a modified technique is currently being optimized in which a vacuum is applied on 1 side of the channels so that the capillary filling speed can be increased and hence longer waveguides can be obtained.

B. Bragg Grating Reflection Spectrum

The Bragg reflection wavelength λ_B is given by:

$$\lambda_B = \frac{2 \cdot n_{eff} \cdot \Lambda}{N},$$

where N is the reflection order ($N = 2$ in this letter), Λ is the pitch of the grating and n_{eff} the effective index of the waveguide mode. The reflection spectrum was determined with the setup shown in Fig 3 using a source with a

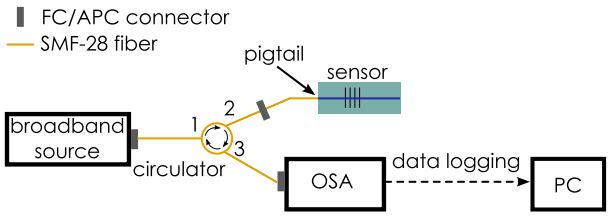

Fig. 3. Setup used to characterize the reflection spectrum of the waveguide Bragg grating sensor.

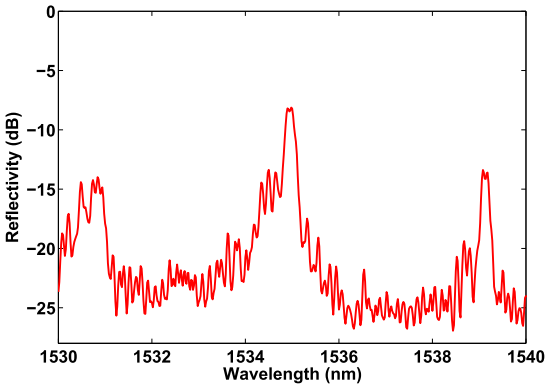

Fig. 4. Reflection spectrum of a 5 µm × 5 µm Ormocer waveguide Bragg grating normalized to the source spectrum (recorded after the pigtailing process; a moving average filter was applied over 5 datapoints).

broadband spectrum from 1530 nm to 1610 nm (ASE FL7002, Thorlabs), a fiber-optic circulator and an Optical spectrum analyzer (OSA). The spectrum obtained was normalized to the source spectrum, yielding actual reflectivity values. To facilitate pigtailing with a standard SMF-28 fiber, slightly larger 5 µm × 5 µm dimensions were chosen, therefore yielding a waveguide supporting a few modes. Fig. 4 shows the reflection spectrum after the pigtailing process revealing 3 peaks (around 1539 nm, 1535 nm and 1531 nm), corresponding with 3 excited modes in the waveguide. Before pigtailing and after optimizing the fiber-to-waveguide alignment, a maximum reflectivity of −6.6 dB (22%) was found. In this reflectivity value also the waveguide losses (estimated to be about 1 dB cm^{-1} for Ormocer around 1550 nm) and fiber-to-waveguide coupling losses (about 1.5 dB per transition) are taken into account. After the pigtailing, the reflectivity slightly reduced due to small alignment shifts during this process.

Although the waveguides were not single mode, a good tracking of the individual peaks was possible owing to the relatively large separation between the peaks and good signal-to-noise ratio.

C. Response to Temperature

The temperature tests were performed in a temperature controlled environmental chamber. The sample was positioned in the center of the chamber and the pigtailed fiber was lead out from a port at the bottom of the chamber. A thermocouple was used to monitor the temperature of the sample. The temperature test cycle was performed between 30 °C and 60 °C. The upper temperature was limited by the stability of the fiber-to-sensor connection. The spectrum acquisition were

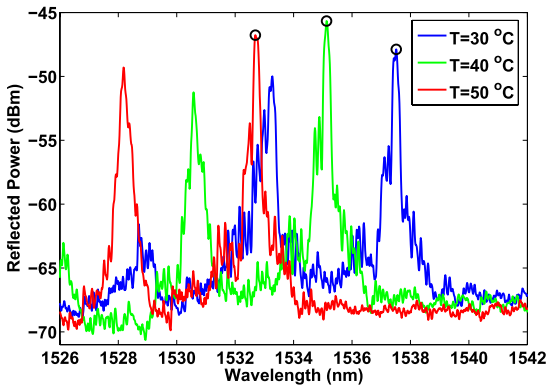

Fig. 5. Reflection spectrum of a 5 µm × 5 µm Ormocer waveguide Bragg grating at different temperatures as obtained from the interrogator. The peak at the longest wavelength (marked with a circle) was tracked during the temperature test.

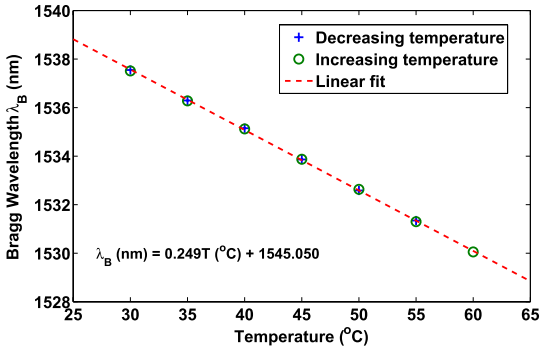

Fig. 6. Relation between Bragg wavelength and temperature (measured data and linear fit).

performed every 5 °C after letting the temperature stabilize in the chamber. In order to check the stability of the measurements, each plateau temperature was maintained stable for 15 minutes and the spectrum was recorded every 5 minutes (3 times for each plateau) showing a good overlap of the signal. The reflection spectrum was tracked using a similar configuration as shown in Fig 3, in which the source, circulator and OSA were replaced by a dedicated optical fiber sensor interrogator (FBGS FBG-Scan808D) operating from 1510 nm to 1590 nm.

Fig. 5 illustrates the blue-shifting of the reflection spectrum at increasing temperature. The reflection peak marked with a circle in the figure was tracked during the thermal test and the corresponding reflection wavelength is plotted with respect to temperature in Fig. 6. The 3 dB bandwidth of this peak was calculated to be around 0.3 nm. We can clearly observe a blue-shift of the selected peak with temperature, and also notice that the results for ramping up or down the temperature match well, showing no clear effect of hysteresis. The linear fit of the data points results in the following relation:

$$\lambda\ (nm) = -0.249\ (nm/^{\circ}C) \times T\ (^{\circ}C) + 1545.050\ (nm)$$

leading to a sensitivity ($\Delta\lambda/\Delta T$) of −249 pm °C^{-1}. Compared to the typical sensitivity of silica fiber Bragg gratings (≈10 pm °C^{-1} around room temperature [1], [4]), this is about 25 times higher.

The (relative) sensor sensitivity to temperature can be expressed as [1]:

$$\frac{\Delta\lambda}{\lambda_{B,0}} = (\alpha + \xi)\,\Delta T,$$

where $\lambda_{B,0}$ is the (second order) Bragg wavelength at reference temperature (25 °C), α is the thermal expansion coefficient and ξ the thermo-optic coefficient.

For the peak at the longest wavelength ($\lambda_{B,0} = 1539\,\text{nm}$), this results in:

$$\frac{\Delta\lambda}{\lambda_0 \Delta T} = (\alpha + \xi) \cong -162\text{ppm/°C}.$$

According to the manufacturer's data, the thermal expansion coefficient (CTE or α) is both for Ormocore and Ormoclad between 100ppm/°C and 130ppm/°C [20], and the thermo-optic coefficient (ξ) is about −250ppm/°C for Ormocore and about −270ppm/°C for Ormoclad, leading to a theoretical relative sensitivity ($\alpha + \xi$) between −120ppm/°C and −170ppm/°C which is in good agreement with the result obtained.

IV. Conclusions

An Ormocer-based waveguide Bragg grating temperature sensor, with a 25-times higher temperature sensitivity than a typical silica fiber was presented. Ormocer, a hybrid inorganic-organic material was chosen owing to its relatively low loss from visible to telecom wavelengths, good thermal stability and high thermo-optic coefficient. Both the gratings and the waveguide required for constructing the sensor were fabricated using a replication-based method. The gratings (1010 nm pitch, second order grating around telecom wavelengths) were imprinted in the under-cladding layer and the waveguide cores were patterned on top by capillary filling of micro-channels which were defined in a transparent and flexible mold. The advantage of this technique is that waveguides are formed only where the micro-channels are present in the mold, therefore requiring very little material and avoiding a residual core layer between neighboring waveguides. Owing to the replication step, the quality and exact dimensions of the waveguides will be determined by the quality of the mold (which can be very high). This means that this technique allows fabrication of waveguides with good quality, even using materials that are difficult to process, e.g. when they are not directly compatible with standard photo-lithography.

To facilitate pigtailing to a standard SMF-28 fiber, the waveguides in the current sensor where chosen slightly larger (i.e. 5 μm × 5 μm) than the dimensions required for single mode operation. Therefore, three clear reflection peaks were found corresponding to the different waveguide modes excited in the slightly multimode waveguide. With optimized fiber-to-waveguide alignment, a maximum reflectivity of −6.6 dB (22%) was obtained and although this value slightly reduced during the pigtailing process, precise peak tracking was possible using a standard interrogator. The peak at the longest wavelength ($\lambda_{B,0} = 1539\,\text{nm}$, corresponding to the fundamental mode) was tracked during temperature testing and a high sensitivity of $-249\,\text{pm}\,°\text{C}^{-1}$ was found.

References

[1] Q. Yu, Y. Zhang, Y. Dong, Y. P. Li, C. Wang, and H. Chen, "Study on optical fiber Bragg grating temperature sensors for human body temperature monitoring," in *Proc. Symp. Photon. Optoelectron. (SOPO)*, May 2012, pp. 1–4.

[2] A. Bar-Cohen, B. Han, and K. J. Kim, "Thermo-optic effects in polymer Bragg gratings," in *Micro- and Opto-Electronic Materials and Structures: Physics, Mechanics, Design, Reliability, Packaging*, E. Suhir, Y. C. Lee, and C. Wong, Eds. New York, NY, USA: Springer, 2007, pp. A65–A110.

[3] Z. Zhang, P. Zhao, P. Lin, and F. Sun, "Thermo-optic coefficients of polymers for optical waveguide applications," *Polymer*, vol. 47, no. 14, pp. 4893–4896, Jun. 2006.

[4] T. Mizunami, H. Tatehata, and H. Kawashima, "High-sensitivity cryogenic fibre-Bragg-grating temperature sensors using Teflon substrates," *Meas. Sci. Technol.*, vol. 12, no. 7, p. 914, 2001.

[5] L. J. Salazar-Serrano, D. Barrera, W. Amaya, S. Sales, V. Pruneri, and J. P. Torres. (2015). "Enhancement of the sensitivity of a temperature sensor based on fiber Bragg gratings via weak value amplification." [Online]. Available: http://arxiv.org/abs/1506.01791.

[6] K. E. Carroll, C. Zhang, D. J. Webb, K. Kalli, A. Argyros, and M. C. J. Large, "Thermal response of Bragg gratings in PMMA microstructured optical fibers," *Opt. Exp.*, vol. 15, no. 14, pp. 8844–8850, Jul. 2007.

[7] G. Statkiewicz-Barabach, K. Tarnowski, D. Kowal, P. Mergo, and W. Urbanczyk, "Fabrication of multiple Bragg gratings in microstructured polymer fibers using a phase mask with several diffraction orders," *Opt. Exp.*, vol. 21, no. 7, pp. 8521–8534, Apr. 2013.

[8] X. Hu, C.-F. J. Pun, H.-Y. Tam, P. Mégret, and C. Caucheteur, "Highly reflective Bragg gratings in slightly etched step-index polymer optical fiber," *Opt. Exp.*, vol. 22, no. 15, pp. 18807–18817, Jul. 2014.

[9] W. Qiu, X. Cheng, Y. Luo, Q. Zhang, and B. Zhu, "Simultaneous measurement of temperature and strain using a single Bragg grating in a few-mode polymer optical fiber," *J. Lightw. Technol.*, vol. 31, no. 14, pp. 2419–2425, Jul. 15, 2013.

[10] A. Lacraz, M. Polis, A. Theodosiou, C. Koutsides, and K. Kalli, "Femtosecond laser inscribed Bragg gratings in low loss CYTOP polymer optical fiber," *IEEE Photon. Technol. Lett.*, vol. 27, no. 7, pp. 693–696, Apr. 1, 2015.

[11] I. P. Johnson *et al.*, "Optical fibre Bragg grating recorded in TOPAS cyclic olefin copolymer," *Electron. Lett.*, vol. 47, no. 4, pp. 271–272, 2011.

[12] W. Yuan *et al.*, "Humidity insensitive TOPAS polymer fiber Bragg grating sensor," *Opt. Exp.*, vol. 19, no. 20, pp. 19731–19739, Sep. 2011.

[13] B. Van Hoe, E. Bosman, J. Missinne, S. Kalathimekkad, G. Van Steenberge, and P. Van Daele, "Novel coupling and packaging approaches for optical interconnects," *Proc. SPIE*, vol. 8267, pp. 82670T-1–82670T-11, Feb. 2012.

[14] B. Van Hoe *et al.*, "Ultra small integrated optical fiber sensing system," *Sensors*, vol. 12, no. 9, pp. 12052–12069, 2012.

[15] L. Eldada *et al.*, "Thermooptic planar polymer Bragg grating OADMs with broad tuning range," *IEEE Photon. Technol. Lett.*, vol. 11, no. 4, pp. 448–450, Apr. 1999.

[16] B. Yun, G. Hu, and Y. Cui, "Third-order polymer waveguide Bragg grating array by using conventional contact lithography," *Opt. Commun.*, vol. 330, pp. 113–116, Nov. 2014.

[17] Y. Binfeng, H. Guohua, and C. Yiping, "Polymer waveguide Bragg grating Fabry–Perot filter using a nanoimprinting technique," *J. Opt.*, vol. 16, no. 10, p. 105501, 2014.

[18] F. Song, J. Xiao, A. J. Xie, and S.-W. Seo, "A polymer waveguide grating sensor integrated with a thin-film photodetector," *J. Opt.*, vol. 16, no. 1, p. 015503, 2014.

[19] M. Wang *et al.*, "Fabrication of optical inverted-rib waveguides using UV-imprinting," *Microelectron. Eng.*, vol. 88, no. 2, pp. 175–178, Feb. 2011.

[20] *OrmoCore and OrmoClad Datasheet From Micro Resist Technology*. [Online]. Available: http://www.microresist.de/en/products/hybrid-polymers/uv-lithography/ormocore-and-ormoclad, accessed Feb. 26, 2016.